onto the guide via a waveguide transition [10]. The insertion loss of two transitions and a straight section of guide having equal length as that used in the coupler was first measured. Thus, power at the coupler ports was corrected for noncoupler losses. The theoretical and experimental behavior of the coupler is shown in Fig. 4.

Fig. 5 illustrates the coupling ratio achieved using dielectric guide of cross section 5.5×5.5 mm and $\epsilon_{r1} = 2.1$ with the same alumina film. An isolation better than 25 dBs was achieved throughout. In both cases, the guide cross-sectional dimensions [9] were calculated to be as large as possible while still supporting only monomode propagation at 40 GHz.

V. Conclusion

The measurements show that over the entire band 26–40 GHz a 2.5-dB coupler has been constructed in image guide. The variation in coupling coefficient was within ± 0.4 dB of the average value, i.e., 2.5 dB. The output at the isolated port was at least 20 dB down over this range. The theoretical model predicted a 2-dB coupling coefficient, with 4.33 dB for the through port. It was found in practice that the dielectric film in the coupler did not make perfect contact with the ground plane and this resulted in more power going to the through port and less to the coupled port. This problem did not occur in the dielectric waveguide as there is no ground plane.

The broad-band performance can be attributed to the fact that coupling takes place in the thin dielectric film, and so these couplers will be much smaller than forward-wave couplers. Also, the small size reduces the overall attenuation of the circuitry.

Appendix

The approximation that a well-guided first-order image or dielectric guide mode is equivalent to a plane wave propagating along the longitudinal axis of the guide follows directly from the Knox and Toulios [9] analysis. In this, the guiding structure is simplified to an infinite slab having an effective dielectric constant. Two plane waves can be used to represent the slab guide TE or TM modes and these will be incident on the two slab boundaries at the same angle $90 - \phi°$, which is greater than the critical angle. Hence, the angles of incidence of the two waves on a dielectric film oriented at 45° to the longitudinal axis and $45 + \phi°$ and $45\text{-}\phi°$, their reflection coefficients being $\rho_{45+\phi}$, $\rho_{45-\phi}$.

The overall reflection coefficient ρ_T for the mode is given by

$$\rho_T = \frac{1}{2}\rho_{45+\phi} + \frac{1}{2}\rho_{45-\phi}. \tag{A1}$$

Provided ϕ is small, which will be the case for a guide with low dielectric constant (even lower effective dielectric constant) and well-guided mode, then

$$\rho_T \approx \rho_{45}. \tag{A2}$$

Otherwise, ϕ must be evaluated from

$$\phi = \tan^{-1}\left(\frac{K_x}{K_z}\right) \tag{A3}$$

where K_z, K_x are the longitudinal and transverse propagation constants, respectively, in the slab; and Al used in the design routine.

Acknowledgment

This work has been supported by a Department of Industry grant. The authors wish to thank E. J. Griffin, R.S.R.E. Malvern, R. W. Yell, and N. P. L. Teddington who have co-supervized this project.

References

[1] E. A. Marcatili, "Dielectric rectangular waveguide and directional coupler for integrated optics," *Bell Syst. Tech. J.*, vol. 48, no. 7, pp. 2071–2102, 1969.
[2] T. Trinh and R. Mittra, "Coupling characteristics of planar dielectric waveguides of rectangular cross section," *IEEE Trans. Microwave Theory Tech.*, vol. MTT-29, pp. 875–880, Sept. 1981.
[3] I. J. Bahl and P. Bhartia, "Aperture coupling between dielectric image lines," *IEEE Trans. Microwave Theory Tech.*, vol. MTT-29, pp. 891–896, Sept. 1981.
[4] R. D. Birch and R. J. Collier, "A broadband image guide directional coupler," in *10th Eur. Microwave Conf.*, (Warsaw), 1980, pp. 295–298.
[5] K. Solbach, "The calculation and the measurement of the coupling properties of dielectric image lines of rectangular cross section," *IEEE Trans. Microwave Theory Tech.*, vol. MTT-27, pp. 54–58, Jan. 1979.
[6] M. Born and E. Wolf, *Principles of Optics*. London: Pergamon Press, 1975, sec. 7.6.
[7] R. Rudokas and T. Itoh, "Passive millimeter-wave IC components made of inverted strip dielectric waveguides," *IEEE Trans. Microwave Theory Tech.*, vol. MTT-24, pp. 978–981, Dec. 1976.
[8] W. D. Burnside and K. W. Burgener, "High frequency scattering by a thin lossless dielectric slab," *IEEE Trans. Antennas Propagat.*, vol. AP-31, pp. 104–110, Jan. 1983.
[9] R. M. Knox and P. P. Toulios, "Integrated circuits for the millimeter through optical frequency range," in *Proc. Symp. Submillimeter-Waves*, Polytechnic Press of Polytechnic Institute of Brooklyn, 1970, pp. 497–516.
[10] R. J. Collier and G. X. Chang, "A broad-band waveguide to image guide transition," in *12th Eur. Microwave Conf.*, 1982, pp. 526–533.

An Iterative Moment Method for Analyzing the Electromagnetic Field Distribution inside Inhomogeneous Lossy Dielectric Objects

MICHEL F. SULTAN, MEMBER, IEEE, AND RAJ MITTRA, FELLOW, IEEE

***Abstract*—An iterative method is proposed for solving the electromagnetic deposition inside lossy inhomogeneous dielectric bodies. The technique uses the conventional method of moments to formulate the problem in matrix form. The resulting system of linear equations is solved iteratively by the method of conjugate gradients.**

The main advantage of the method is that the iterative procedure does not require the storage of any matrix, thus offering the possibility of solving larger problems compared to conventional inversion or Gaussian elimination schemes. Another important advantage is that monotonic convergence to a solution is ensured and accomplished within a fixed number of iterations, not exceeding the total number of basis functions, independently of the initial guess for the solution.

Preliminary examples involving two-dimensional cylinders of fat and muscle are illustrated. The iterative method is extendable and applicable to the three-dimensional case.

Manuscript received February 13, 1984; revised September 17, 1984. This work was supported in part by the National Science Foundation, NSF ECS 81-20305 and the Office of Naval Research, N00014-81-K-0245.

The authors are with the Electrical Engineering Department, University of Illinois, Urbana, IL.

0018-9480/85/0002-0163$01.00 ©1985 IEEE

I. Introduction

An important problem in the electromagnetic heating of deep-seated tumors, or hyperthermia, is the determination of the electromagnetic field distribution and power deposition inside illuminated lossy inhomogeneous dielectric bodies. Analytical techniques that guarantee a unique and exact solution are applicable for simple geometries only. For approximate solutions of a wider range of problems, many numerical or asymptotic techniques are available, including the method of moments [1]–[3], the finite-element method [4], the extended boundary condition method and its iterative version [5]–[7], and the geometrical theory of diffraction [8].

For reasonably accurate modeling of many problems of interest, numerical techniques such as the method of moments usually require a large number of basis functions, thus leading to large matrix equations often exceeding the storage capability of the computer. For these problems, the resulting system of linear equations cannot be solved by conventional methods that require the storage of the matrix, such as in complete matrix inversion, Gaussian elimination, or LU decomposition. This type of limitation is usually encountered in problems where the electromagnetic field distribution is to be determined in biological bodies in the resonance and post-resonance frequency range.

Iterative techniques offer the possibility of solving large systems of equations without requiring the storage of any matrices. In a survey of numerical techniques for the solution of large systems of linear equations, Sarkar *et al.* [9] enumerate the relative advantages and disadvantages of the various popular iterative methods. One of the best available techniques at present is the method of conjugate gradients, where a finite number of iterations, usually less than the order of the matrix, is sufficient to obtain the desired solution [10].

In this paper, we apply the method of conjugate gradients to extend that range of the method of moments to larger problems. The study is confined to the characterization of the electromagnetic field distribution inside two-dimensional inhomogeneous lossy cylinders illuminated by a TM plane wave. The same procedure applies for the more general three-dimensional case also. In this approach, the computer storage requirements are proportional to the total number of unknowns only, and not to the square of that number, as required by many of the conventional techniques for solving linear equations.

The method of conjugate gradients is a versatile mathematical tool that can be used to supplement and increase the range of the method of moments, as demonstrated here, as well as of many other existing numerical methods for solving electromagnetic problems. This type of iterative technique has been recently applied to several electromagnetic problems involving perfect conductors [11]–[13] and dielectric bodies as well [14], [15].

II. Formulation by the Method of Moments

Consider the two-dimensional inhomogeneous dielectric cylinder of arbitrary cross section illustrated in Fig. 1. The cylinder is illuminated by an incident TM plane wave E^i. Both the incident field and the induced polarization current have only a z component. The polarization current satisfies the integral equation [1], [16]

$$\frac{J(x,y)}{j\omega\epsilon_0(\epsilon_r(x,y)-1)}+\frac{kn}{4}\iint_{S_D}J(x',y')\,H_0^{(2)}(k|\rho-\rho'|)\,dx'\,dy' = E^i(x,y) \quad (1)$$

where the complex relative permittivity ϵ_r is inhomogeneous only in the transverse coordinates, S_D is the support of the dielectric cylinder, $H_0^{(2)}$ is the Hankel function of the second kind, zero order, and where

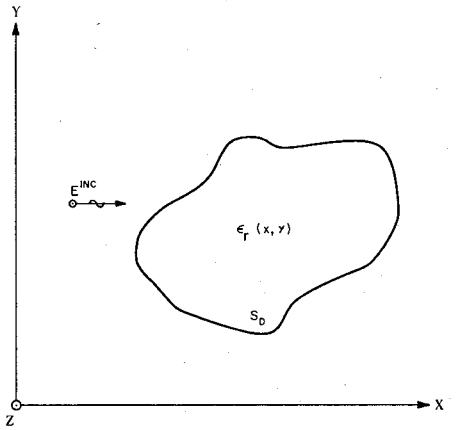

Fig. 1. Cross section of an arbitrarily shaped two-dimensional lossy-inhomogeneous dielectric cylinder illuminated by a TM plane wave.

$$|\rho-\rho'|=\sqrt{(x-x')^2+(y-y')^2}. \quad (2)$$

The application of the method of moments converts the integral equation (1) into a matrix equation, where the polarization current is the unknown vector to be determined

$$\underline{\underline{Z}}\,\underline{J}=\underline{E}^i. \quad (3)$$

Matrix equations resulting from application of the method of moments are usually solved by conventional direct methods including matrix inversion, Gaussian elimination, and LU decomposition. The approach that will be used in this paper to solve the matrix equation (3) is based on an iterative process, known as the method of conjugate gradients, where the matrix elements are not stored, but are generated repeatedly as needed during each iteration. It is thus important to find the most efficient way to generate the matrix elements. In this initial study, we have chosen to use the simplest basis and testing functions, pulse and delta functions, respectively, because this choice allows us to compute the matrix elements in a very efficient manner. However, in some cases, it may be more advantageous to use a smaller number of higher order functions, although the computation of each matrix element will be less efficient.

The cross section of the dielectric cylinder is divided into a total of N cells, where each cell is chosen small enough to ensure uniformity of the current. When the integral equation (1) is enforced at the center of each cell, the resulting expressions for the elements of the impedance matrix $\underline{\underline{Z}}$ are obtained and are given by

$$Z_{pq}=\frac{1}{j\omega\epsilon_0(\epsilon_r(x_p,y_p)-1)}+\frac{k\eta}{4}\iint_{S_q}H_0^{(2)}(k|\rho_p-\rho_q|)\,dx_q\,dy_q \quad (4)$$

where S_q is the area of the qth cell. An approximation to the integral in (4) is obtained by assuming that cell q is circular with radius a_q given by

$$a_q=\left(\frac{S_q}{\pi}\right)^{1/2}. \quad (5)$$

With this assumption, the approximation to the integral is obtained analytically [1]. The resulting approximate expressions for

the impedance matrix elements are given by

$$Z_{pq}=\begin{cases}\eta\left[\dfrac{\epsilon_r(x_p,y_p)}{jk(\epsilon_r(x_p,y_p)-1)}+\dfrac{\pi a_p}{2}H_1^{(2)}(ka_q)\right], & p=q\\ \eta\dfrac{\pi a_q}{2}J_1(ka_q)H_0^{(2)}(k|\rho_p-\rho_q|), & p\neq q\end{cases} \tag{6}$$

where J_1 and $H_1^{(2)}$ are the Bessel function, order one, and the Hankel function of the second kind, order one, respectively.

The computational time for the off-diagonal elements can be reduced by scaling the matrix equation (3) in the following way:

$$\boldsymbol{Z}'\underline{J}'=\underline{E}^i \tag{7}$$

where

$$\underline{J}'=\operatorname{diag}\left\{\eta\frac{\pi}{2}a_qJ_1(ka_q)\right\}\underline{J}. \tag{8}$$

The matrix equation (7) is solved for $\underline{J}'$. After rescaling the polarization current, the total electric field can be obtained by application of the constitutive relationship

$$E(x_q,y_p)=\frac{J(x_p,y_p)}{j\omega\epsilon_0(\epsilon_r(x_p,y_p)-1)}. \tag{9}$$

III. Iterative Solution by the Method of Conjugate Gradients

The basic principles behind the method of conjugate directions, in general, and the method of conjugate gradients, in particular, are described in an original paper by Hestenes and Stiefel [10]. For the solution of any complex matrix equation $\boldsymbol{A}\underline{x}=\underline{b}$, the method of conjugate gradients starts with an initial guess for $\underline{x}$, $\underline{x}^{(0)}$, and generates the residual vector

$$\underline{R}^{(0)}=\boldsymbol{A}\underline{x}^{(0)}-\underline{b} \tag{10}$$

and the direction vector

$$\underline{P}^{(1)}=-\boldsymbol{A}^*\underline{R}^{(0)} \tag{11}$$

where $\boldsymbol{A}^*$ is the complex conjugate transpose of $\boldsymbol{A}$. The iterative process starts at this point, and proceeds as follows for the nth iterative step:

$$\alpha_n=\frac{\|\boldsymbol{A}^*\underline{R}^{(n-1)}\|^2}{\|\boldsymbol{A}\underline{P}^n\|^2}=\frac{\langle\boldsymbol{A}^*\underline{R}^{(n-1)},(\boldsymbol{A}^*R^{(n-1)})^*\rangle}{\langle\boldsymbol{A}\underline{P}^n,(\boldsymbol{A}\underline{P}^n)^*\rangle} \tag{12}$$

$$\underline{x}^{(n)}=\underline{x}^{(n-1)}+\alpha_n\underline{P}^{(n)} \tag{13}$$

$$\underline{R}^{(n)}=\underline{R}^{(n-1)}+\alpha_n\boldsymbol{A}\underline{P}^{(n)} \tag{14}$$

$$\beta_n=\frac{\|\boldsymbol{A}^*\underline{R}^{(n)}\|^2}{\|\boldsymbol{A}^*\underline{R}^{(n-1)}\|^2} \tag{15}$$

$$\underline{P}^{(n+1)}=\beta_n\underline{P}^{(n)}-\mathbf{A}^*\underline{R}^{(n)}. \tag{16}$$

It has been demonstrated that, for the case when no rounding-off errors occur, the method of conjugate gradients converges to the exact solution of the matrix equation, in at most N steps, where N is the order of the square matrix $\boldsymbol{A}$ [10]. The iterative algorithm given above applies to any systems $\boldsymbol{A}\underline{x}=\underline{b}$, where $\boldsymbol{A}$ may be a complex nonHermitian matrix, of the type often encountered in electromagnetic problems. In particular, it applies to the matrix equation (7).

In any iterative process, a prespecified criterion has to be selected, such as to terminate the iteration whenever a desired degree of accuracy is present in the solution. In the method of conjugate gradients, one could stop the iteration after N steps, thus making sure that the solution is exact, assuming no appreciable rounding-off errors occur. However, one can terminate the iteration at a much earlier step, while still keeping the degree of accuracy in the solution within acceptable limits. A good and reliable measure of accuracy is believed to be the root-mean-square error per sample, defined as [1]

$$\delta_n=\frac{\langle\underline{R}^{(n)},(\underline{R}^{(n)})^*\rangle^{1/2}}{N}=\frac{\|R^{(n)}\|}{N}. \tag{17}$$

At the nth iterative step, the norm of the residual vector is given by [17]

$$\|\underline{R}^{(n)}\|^2=\|\underline{R}^{(n-1)}\|^2-\frac{\|\boldsymbol{A}^*\underline{R}^{(n-1)}\|^4}{\|\boldsymbol{A}\underline{P}^{(n)}\|^2}. \tag{18}$$

From (18), it is obvious that both the norm of the residual $\|\underline{R}^{(n)}\|$, as well as its normalized value δ_n, are monotonically decreasing quantities.

Another measure of accuracy which may be more meaningful is defined as

$$\gamma_n=\frac{\delta_n}{\|\underline{x}^{(n)}\|/N}=\frac{\|\underline{R}^{(n)}\|}{\|\underline{x}^{(n)}\|}. \tag{19}$$

A value of $\gamma_n=0.001$ means that the degree of accuracy in the solution is *at best* 3 significant digits for all samples. Thus, for 3 significant digits of accuracy, γ_n has to be less than 0.001. A value of 10^{-4} may be a reasonably good choice.

IV. Some Numerical Examples

The matrix equation (7) has been solved iteratively by the method of conjugate gradients for several two-dimensional dielectric problems. After obtaining the solution to (7), the polarization current is computed from (8). The matrix elements are never stored. To speed up the computational time for the matrix elements, a look-up table for the Hankel function of the second kind, order one, is constructed before the initialization of the iterative process. The look-up table is later used to approximate Hankel functions by linear interpolation.

Fig. 2(a) and (b) illustrates the normalized current density on a 40-cm strip of muscle, induced by a plane TM wave at 915 MHz, normal incidence (Fig. 2(a)), and grazing incidence (Fig. 2(b)). For each case, the same current distribution is observed whether the strip is divided into 100, 75, or 50 cells. In both cases, satisfactory results are also obtained when the strip is divided in 25 cells only. Similar observations are made for a 100-cm fat strip with normal incident (Fig. 3(a)) and grazing incident (Fig. 3(b)) TM fields at 915 MHz. However, for the case of normal incidence, the strip must be divided into more than 25 cells for satisfactory results (Fig. 3(a)).

Inhomogeneous problems involving both fat and muscle have also been solved by the same approach. Fig. 4(a) and (b) illustrates the polarization current induced on a 90-cm strip of fat and muscle, illuminated by a 915-MHz plane TM wave at normal incidence (Fig. 4(a)), and grazing incidence (Fig. 4(b)). Relative to the coordinates system used, the fat–muscle interface x_{FM} is located at 0 cm (all muscle), 30 cm (one-third fat, two-thirds muscle), 60 cm (two-thirds fat, one-third muscle), and 90 cm (all fat). For the normal incidence case, and for the cases where x_{FM}

[1] Note that other normalizations for the definition of δ_n are also possible and that the choice of the normalization does not affect the variation of δ_n with iteration.

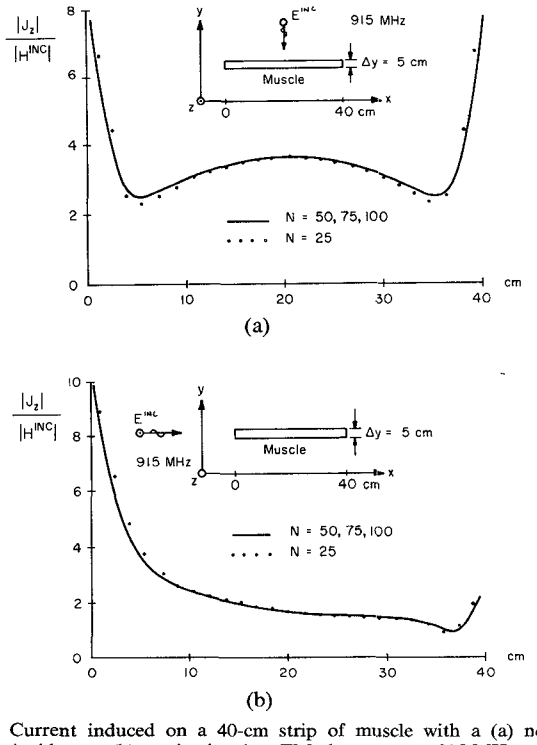

Fig. 2. Current induced on a 40-cm strip of muscle with a (a) normally incident or (b) grazing incident TM plane wave at 915 MHz.

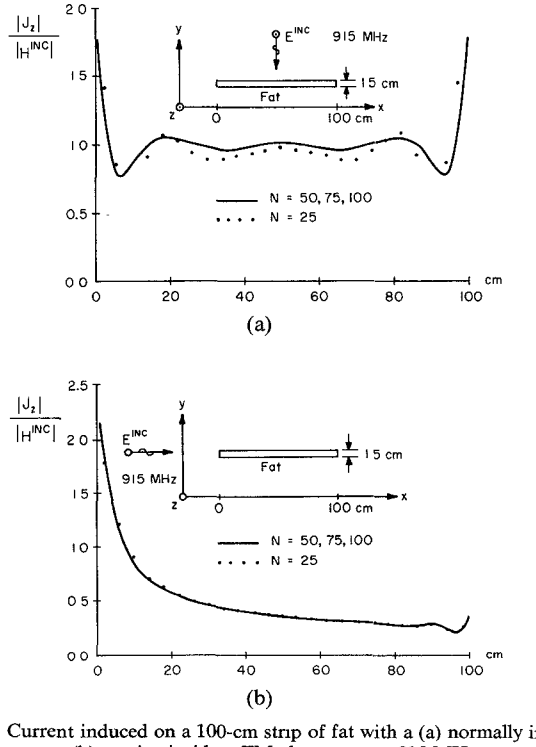

Fig. 3. Current induced on a 100-cm strip of fat with a (a) normally incident or (b) grazing incident TM plane wave at 915 MHz.

is located at 30 cm or 60 cm, the current induced in the fat portion, away from the interface, is identical to the current that is induced in a homogeneous strip of fat. Similarly, the current induced in the muscle portion, away from the interface, is identical to the current induced in a homogeneous strip of muscle (Fig. 4(a)). The shape and magnitude of the current distribution at and near the interface are the same, whether the interface is located at 30 cm or 60 cm (Fig. 4(a)). It is interesting to note that the

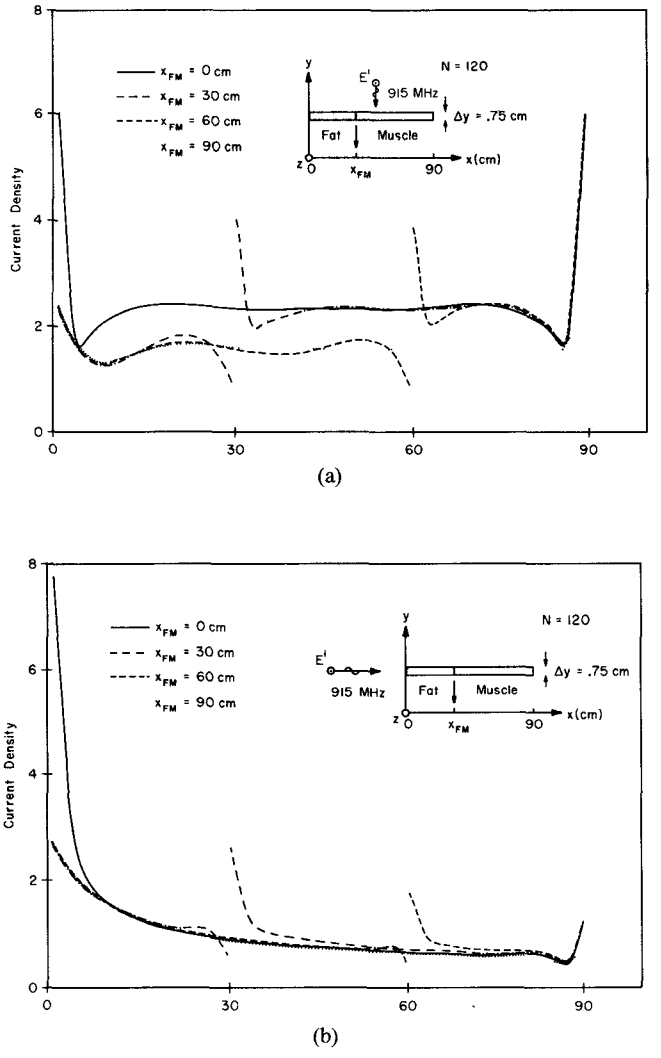

Fig. 4. (a) Polarization current induced on a 90-cm strip of fat and muscle illuminated by a 915-MHz plane TM wave at normal incidence. (b) Polarization current induced on a 90-cm strip of fat and muscle illuminated by a 915-MHz plane TM wave at grazing incidence.

portion over which the disturbance in the current distribution is created by the presence of the interface is roughly equal to one wavelength in free space, 32.8 cm. For the grazing incidence case, the shape of the current distribution at and near the interface is the same, while the magnitude is smaller for the case where the interface is located at 60 cm, because of the attenuation of the wave as it travels through the extra 30-cm strip of fat (Fig. 4(b)).

More complicated inhomogeneous problems have also been solved iteratively by the method of conjugate gradients. Fig. 5(b) shows the current induced in the cylindrical structure illustrated in Fig. 5(a). This problem is first solved on a CDC Cyber 175 computer using a total of 216 samples, with zero for initial guess. The root-mean-square error per sample δ_n is plotted in the first portion of the lower curve in Fig. 5(c). The solution is then used as an initial guess to solve the same problem with finer sampling in muscle, with a total of 432 samples. The root-mean-square error per sample for this case is illustrated in the second portion of the lower curve in Fig. 5(c). A much longer computational time would have been required had we started with zero for initial guess, as illustrated in the upper curve of Fig. 5(c). There is no significant difference in the current distributions for the cases of 216 and 432 samples.

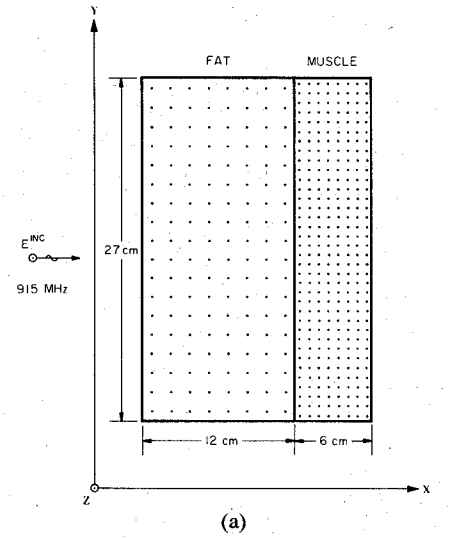

(a)

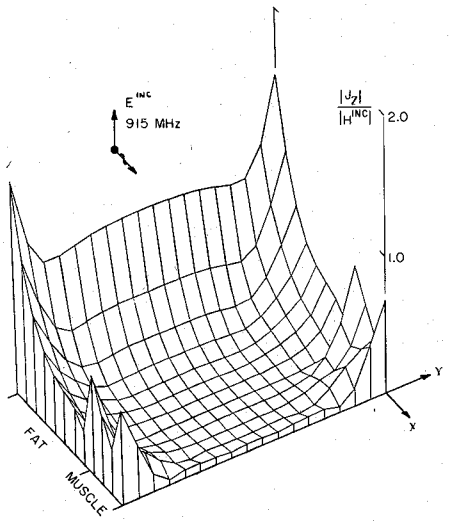

(b)

Fig. 5. (a)Two-dimensional rectangular cylinder containing both fat and muscle, illuminated by a normally incident TM plane wave at 915 MHz. (b) A view of the current induced in the structure shown in Fig. 5(a). (c) Convergence of the method of conjugate gradients when solving for the current induced in the structure shown in Fig. 5(a): the root-mean-square error per sample as a function of CPU time.

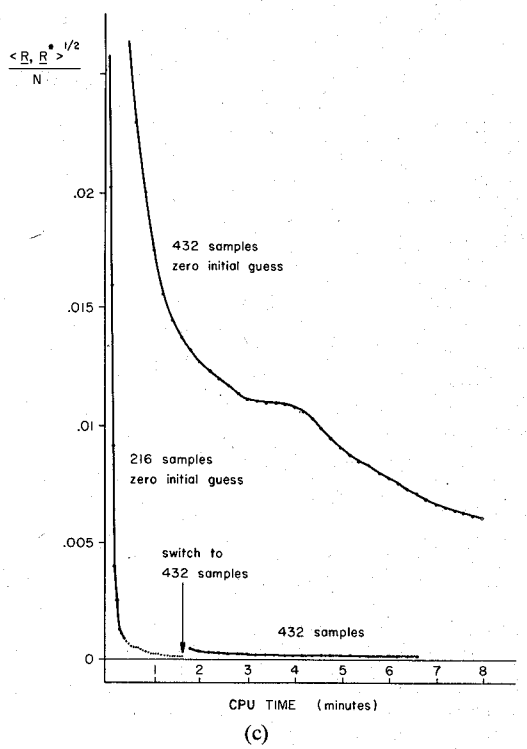

(c)

Fig. 5. (*Continued*)

V. Concluding Remarks

The problem of electromagnetic field distribution inside inhomogeneous lossy dielectrics is formulated in matrix form by the method of moments, with pulse basis functions and point matching. The resulting system of N linear equations is solved iteratively by the method of conjugate gradients. Since no matrix elements are stored, the computer storage requirements are considerably less than is required in conventional inversion, Gaussian elimination, or LU decomposition schemes. The storage requirement for these conventional schemes is usually of the order of N^2, compared to $5N$ for the method of conjugate gradients. With a clear saving in computer storage space, the iterative approach offers the possibility of solving larger problems, at the expense of more computational time to generate the matrix elements.

Another advantage of the method is that the iterative process is guaranteed to converge monotonically to a solution in at most N steps, regardless of the initial guess, with the option of terminating the iteration automatically, once a prespecified criterion has been met. The criterion for stopping the iterative process is based on the fact that the norm of the residual vector is a monotonically decreasing quantity.

In the numerical solution of large systems of linear equations, one is confronted with the possibility that the computed results may be severely contaminated by the accumulation of rounding-off errors. In the method of conjugate gradients, one has the option of checking whether appreciable rounding-off errors have accumulated, by computing the residual vector directly, at the completion of the final iteration, $\underline{R}^{(f)} = \underline{Z}\underline{J}^{(f)} - \underline{E}^i$, and comparing the result with the residual vector that has been updated through the iterative process as in (14).

As has been mentioned already, convergence of the method of conjugate gradients does not depend on the initial guess. However, referring to Fig. 5(c), it is possible in some cases to save a considerable amount of computer time by starting with a good initial guess, even when the computational time to obtain this guess is accounted for.

As presented here, the method of conjugate gradients is not by itself a method to solve electromagnetic problems. Instead, it is presented as a mathematical tool that can be used to supplement and increase the range of many existing methods, the method of moments being just one of them. It is, however, possible to apply the method of conjugate gradients directly to integrodifferential operator equations without the intermediate step of formulating a specific matrix equation by any conventional method, as has been demonstrated recently by other authors [11], [12], [14], [15].

References

[1] J. H. Richmond, "Scattering by a dielectric cylinder of arbitrary cross-section shape," *IEEE Trans. Antennas Propagat.*, vol. AP-13, pp. 334–341, 1965.

[2] D. E. Livesay and K. M. Chen, "Electromagnetic fields induced inside arbitrarily shaped biological bodies," *IEEE Trans. Microwave Theory Tech.*, vol. MTT-22, pp. 1273–1280, 1974.

[3] K. M. Chen and B. S. Guru, "Internal EM field and absorbed power density in human torsos induced by 1–500-MHz EM waves," *IEEE Trans. Microwave Theory Tech.*, vol. MTT-25, pp. 746–756, 1977.

[4] M. A. Morgan and K. K. Mei, "Finite-element computation of scattering by dielectric resonator of very high permittivity," *IEEE Trans. Microwave Theory Tech.*, vol. MTT-23, pp. 199–208, 1975.
[5] P. W. Barber, "Scattering and absorption efficiencies for nonspherical dielectrical objects—Biological models," *IEEE Trans. Biomed. Eng.*, vol. BME-25, pp. 155–159, 1978.
[6] M. F. Iskander, A. Lakhtakia, and C. H. Durney, "A new procedure for improving the solution stability and extending the frequency range of the EBCM," *IEEE Trans. Antennas Propagat.*, vol. AP-31, pp. 317–324, 1983.
[7] A. Lakhtakia, M. F. Iskander, and C. H. Durney, "An iterative extended boundary condition method for solving the absorption characteristics of lossy dielectric objects of large aspect ratios," *IEEE Trans. Microwave Theory Tech.*, vol. MTT-31, pp. 640–647, 1983.
[8] T. Isihara and L. B. Felsen, "High-frequency fields excited by a line source located on a concave cylindrical impedance surface," *IEEE Trans. Antennas Propagat.*, vol. AP-27, pp. 172–179, 1979.
[9] T. K. Sarkar, K. R. Siarkiewick, and R. F. Stratton, "Survey of numerical methods for solution of large systems of linear equations for electromagnetic field problems," *IEEE Trans. Antennas Propagat.*, vol AP-29, pp. 847–856, 1981.
[10] M. R. Hestenes and E. Stiefel, "Methods of conjugate gradients for solving linear systems," *J. Res. Nat. Bur. Stand.*, vol. 49, pp. 409–436, 1952.
[11] T. K. Sarkar and S. M. Rao, "The application of the conjugate gradient method for the solution of electromagnetic scattering from arbitrarily oriented wire antennas," in *Proc. Int. URSI Symp.*, (Spain), 1983, pp. 93–96.
[12] T. K. Sarkar, "The applications of the conjugate gradient method for the solution of transient scattering," in *Proc. Int. URSI Symp.*, (Spain), 1983, pp. 215–217.
[13] M. F. Sultan and R. Mittra, "Scattering from large smooth-cornered conducting cylinders," manuscript in preparation.
[14] P. M. Van den Berg, "Iterative computational techniques in scattering based upon the integrated square error criterion," in *Proc. Int. URSI Symp.*, (Spain), 1983, pp. 97–100.
[15] P. M. Van den Berg, A. T. DeHoop, A. Segal, and N. Praagman, "A computational model of the electromagnetic heating of biological tissue with application to hyperthermic cancer therapy," *IEEE Trans. Biomed. Eng.*, vol. BME-30, pp.797–805, Dec. 1983.
[16] R. F. Harrington, *Field Computation by Moment Methods*. Malabar, FL: R. E. Krieger, 1982.
[17] M. F. Sultan and R. Mittra, "Iterative methods for analyzing electromagnetic scattering from dielectric bodies," Electromagnetics Laboratory Report 84-4, University of Illinois at Urbana, Illinois, 1984.

On the Graceful Degradation Performance of Multiple-Device Oscillators

S. SARKAR AND M. C. AGRAWAL

Abstract—**Kurokawa's theory of multiple-device oscillators is extended to an analysis of the graceful degradation performance (GD) of the power-combined oscillators. The analysis shows that the failure of some of the constituent devices of a multiple-device oscillator results in a load-pull effect on the operating devices along with a degradation of power-combining efficiency of the oscillator circuit. A tradeoff exists between power output and circuit improvement of the GD.**

I. Introduction

In many applications, a number of oscillating devices (such as Gunn's, IMPATT's, etc.) are power combined to generate the required level of microwave power [1], [2]. One of the requirements of such multiple-device oscillators is that the power output degrades gracefully as one or more of its constituent devices fail to operate. The graceful degradation performance (GD) is given by the oscillator power output expressed as a fraction of its no-failure power level. It has been observed [1], [3] that in practice the GD is well below the ideal which corresponds to power reduction by just the amount contributed by the failed devices. Saleh [4] and Kinman *et al.* [5] showed that the deviation of the GD from the ideal is in some way connected with the circuitry involved. In this paper, an attempt has been made to identify the factors which govern the GD of multiple-device oscillators.

Manuscript received April 9, 1984; revised August 20, 1984. This work is a part of a research project supported by the University Grants Commission, India, under the Special Assistance Program.

The authors are with the Department of Electronics and Communication Engineering, University of Roorkee, Roorkee-247667, India.

II. Factors of the GD

Typically, a multiple-device oscillator [6] consists of a number N of identical negative conductance devices, each terminated by a conductance G_0 and equally coupled to a power-combining resonator. Fig. 1 shows the coupling between the resonator and one of the devices. Dots signify the existence of the other devices. The device is represented by its negative conductance $-g_D(A_K)$ and susceptance b_D, where A_K is the RF voltage amplitude that the device sees across its terminals $T-T$, when K of devices operate. The resonator is equivalent to a parallel combination of its loss conductance G_C, externally coupled load conductance G_L, a capacitance C, and an inductance L. In Fig. 1, the insert between the device and its terminals $T-T$ shows the effective load conductance $g_L(K)$ and susceptance $b_L(K)$ presented across the device by the entire circuit to the right of $T-T$. Since all the devices are equally coupled to the resonator $(n:1)$ they see the same A_K, $g_L(K)$, and $b_L(K)$.

Assuming that M of the devices belonging to the oscillator described above fail identically and behave as open circuits after failure, it can be shown through Kurokawa's analysis [6], that the GD in decibels is of the form

$$\mathrm{GD} = IDPD + ED + ID, \qquad \text{db} \tag{1}$$

where

$$\mathrm{IDPD} = 10\log_{10}\left[\left(\frac{A_{N-M}}{A_N}\right)^2 \frac{G_C+G_L+n^2G_0N}{G_C+G_L+n^2G_0N(1-M/N)}\right], \quad \text{db} \tag{2}$$

$$\mathrm{ED} = 10\log_{10}\left[\left(1-\frac{M}{N}\right)\frac{G_C+G_L+n^2G_0N}{G_C+G_L+n^2G_0N(1-M/N)}\right], \quad \text{db} \tag{3}$$

$$\mathrm{ID} = 10\log_{10}(1-M/N), \qquad \text{db}. \tag{4}$$

The ratio of load conductance seen by an individual device for $K=N-M$ to that for $K=N$ is [6]

$$\frac{g_L(N-M)}{g_L(N)} = \frac{G_C+G_L+n^2G_0N}{G_C+G_L+n^2G_0N(1-M/N)}. \tag{5}$$

From (2) and (5) it can be easily seen that the individual diode power degradation (IDPD) represents the effect of device failure on the power output of each individual device. In other words, with device failure, the operating devices experience a load-pull effect. From Kurokawa's analysis [6], it also follows that the efficiency degradation (ED) as given by (3) stands for the effect of device failure on the power-combining efficiency of the oscillator circuit. The ideal power degradation (ID) is given by (4). Thus, the factors of the GD are represented by its three components IDPD, ED, and ID.

0018-9480/85/0002-0168$01.00 ©1985 IEEE